Group IV photonic devices for the mid-infrared

G. Mashanovich, M. Nedeljkovic, M. Milosevic, Y. Hu, F. Gardes, et al.

G. Z. Mashanovich, M. Nedeljkovic, M. M. Milosevic, Y. Hu, F. Y. Gardes, D. J. Thomson, T.-B. Masaud, E. Jaberansary, H. M. H. Chong, R. Soref, G. T. Reed, "Group IV photonic devices for the mid-infrared," Proc. SPIE 8431, Silicon Photonics and Photonic Integrated Circuits III, 84310D (10 May 2012); doi: 10.1117/12.922814

SPIE.

Event: SPIE Photonics Europe, 2012, Brussels, Belgium

Group IV photonic devices for the mid-infrared

G. Z. Mashanovich[a], M. Nedeljkovic[a], M. M. Milosevic[b], Y. Hu[a], F. Y. Gardes[a], D. J. Thomson[a], T.-B. Masaud[a], E. Jaberansary[a], H. M. H. Chong[a], R. Soref[c], G. T. Reed[a]
[a]School of Electronics and Computer Science, University of Southampton, Southampton, UK
[b]Department of Electronic Engineering, University of Surrey, Guildford, Surrey, UK
[c]Physics and Engineering Departments, University of Massachusetts at Boston, MA 02125, USA

ABSTRACT

Group IV mid-infrared photonics is attracting more research interest lately. The main reason is a host of potential applications ranging from sensing, to medicine, to free space communications and infrared countermeasures. The field is, however, in its infancy and there are several serious challenges to be overcome before we see progress similar to that in the near-infrared silicon photonics. The first is to find suitable material platforms for the mid-infrared. In this paper we present experimental results for passive mid-infrared photonic devices realised in silicon-on-insulator, silicon-on-sapphire, and silicon on porous silicon. We also present relationships for the free-carrier induced electro-refraction and electro-absorption in silicon and germanium in the mid-infrared wavelength range. Electro-absorption modulation is calculated from impurity-doping spectra taken from the literature, and a Kramers-Kronig analysis of these spectra is used to predict electro-refraction modulation. We examine the wavelength dependence of electro-refraction and electro-absorption, finding that the predictions suggest longer-wave modulator designs will in many cases be different than those used in the telecom range.

Keywords: silicon photonics, mid-infrared, optical modulators, waveguides

1. INTRODUCTION

Mid-infrared group IV photonics has attracted increasing attention in the last few years, driven mainly by the lure of possible applications such as chemical-bio-physico sensing, free-space communications, thermal imaging and infrared countermeasures. Many important gases have their fundamental absorptions in the 3 to 14μm wavelength region, which could be exploited for sensing applications.

Using group IV materials such as silicon and germanium in the mid-infrared is attractive because many of the techniques developed for design, fabrication and testing of telecoms wavelength silicon photonics, which has flourished in recent years, should be readily transferable to longer wavelengths. Potentially the most desirable aspect of this approach is that in future there could be chip-level integration of a mid-infrared system and CMOS electronics, which would enable lab-on-a-chip sensing systems. Richard Soref has previously explored a variety of possible implementations of such systems [1,2].

However there are still significant obstacles associated with the realization of both passive and active mid-infrared components in group-IV materials. Crucially SiO_2, which is used as the insulator in silicon-on-insulator (SOI) waveguides for telecoms wavelength applications, absorbs strongly in most parts of the mid-infrared [3], though it can be used in the 3-4μm range. Therefore alternative material platforms must be explored that have low losses at other mid-infrared wavelengths. Silicon-on-sapphire (SOS) has so far been a popular platform for early investigations, and such waveguides have been demonstrated at 3.4μm [4], 4.5μm [5], 5.18μm [6] and 5.5μm [7]. The drawback of SOS is that sapphire is a very hard material, so samples cannot be polished before measurement to produce optically smooth waveguide facets. Other materials that have been used as a lower cladding layer replacement for SiO_2 with silicon waveguides are porous silicon (SiPSi) [8] and air where silicon waveguides have been undercut by etching [9]. Germanium waveguide material platforms will also be a target for future research, as silicon is only transparent to 8μm because of lattice absorption, whereas germanium is transparent up to around 12μm. In this paper we present our results on SOI, SOS and SiPSi waveguides in the 3-4μm wavelength region.

Optical modulators will be important devices in many active long wave group IV systems. However, existing relationships describing the free-carrier plasma dispersion effect, the most effective modulation mechanism in silicon,

Silicon Photonics and Photonic Integrated Circuits III, edited by Laurent Vivien, Seppo K. Honkanen, Lorenzo Pavesi, Stefano Pelli, Proc. of SPIE Vol. 8431, 84310D · © 2012 SPIE · CCC code: 0277-786X/12/$18 · doi: 10.1117/12.922814

are only valid at the telecoms wavelengths 1.3μm and 1.55μm. We have calculated expressions for electro-absorption and electro-refraction induced by changing free charge-carrier concentrations in silicon for the 1.3-14μm wavelength range. We will present here our calculations, and discuss the implications of our results for longer wave modulator design.

2. EXPERIMENTAL RESULTS

2.1. Waveguide design and fabrication

We have previously reported design rules for single mode and polarization independent SOI rib waveguides for the 3.39μm wavelength [10]. We fabricated rib waveguides that satisfied these design rules, having the following dimensions: height H=2μm, width W=2μm and etch depth D=1.2μm. A buried oxide layer (BOX) thickness of 2μm was used to suppress substrate leakage. We have fabricated such waveguides using standard lithography and reactive ion etching (RIE).

Silicon-on-sapphire strip waveguides were made using the same fabrication process. These silicon strip waveguides had height H=0.6μm and width 2μm, over a sapphire substrate. It was mentioned in the introduction that sapphire cannot be polished using the standard polishing techniques used for silicon or SOI wafers. Therefore when the samples are cleaved the smoothness of the waveguide facets, and therefore coupling efficiency to an optical fiber, is very unreliable. Our solution is therefore to first cleave facets, before using a focused ion beam (FIB) to "trim" the waveguide facets, leaving a smooth profile [4]. To suppress charging of the dielectric substrate the chip was sputtered with a 100nm layer of Al before FIB treatment.

Silicon-on-porous silicon waveguides use porous silicon, which has a lower refractive index than crystalline silicon, as the lower cladding material. SiPSi waveguides were fabricated by proton beam irradiation, using large area ion irradiation with 250keV protons and a fluence of about $1x10^{14}cm^{-2}$ [8]. Following irradiation samples were etched in an HF:water:ethanol solution of ratio 1:1:2, and a two step etching process was performed. From fitting a Bruggeman formula to reflectance spectra a porous silicon refractive index of about 1.4 was measured. The fabricated waveguide dimensions were 4 x 2μm.

2.2. Waveguide characterization

To characterize the waveguides an experimental setup comprising a 3.39μm CW linearly polarized He-Ne laser for the source, mid-infrared fibers for coupling light into the chip and an IRphotonics InSb photodetector was used. We also used a Daylight Solutions tunable quantum cascade laser (3.72-3.90μm) for measurements around the 3.8μm wavelength. This setup is described in greater detail in [8]. To couple light between the optical fibers and waveguides butt coupling was used, and all of the SOI and SOS waveguides had tapers 10μm wide to improve the fiber to waveguide coupling efficiency.

All waveguide propagation losses were measured using the cut-back method, where waveguides of different lengths had been fabricated on the same chip. The bend radii used were 200μm for the SOI waveguides and 40μm for the SOS waveguides. SOI rib waveguide propagation losses were measured at 3.39μm, 3.73μm and 3.80μm. Figure 1 shows the propagation loss measurement results at these three wavelengths. The measured losses were 2.0-2.4dB/cm at 3.39μm, 2.9±0.3dB/cm at 3.73μm and 3.4±0.2dB/cm at 3.80μm. Following these measurements the samples were oxidized with a 20-30nm thick thermal oxide in order to reduce the losses from scattering. They were then remeasured at 3.39μm, and the losses were reduced to 0.6-0.7dB/cm. It is expected that the loss at the two longer wavelengths would be similarly reduced.

Figure 2 shows the propagation loss for SOS waveguides. The measured loss at the wavelength of 3.39μm was 3.6±0.2dB/cm. Figure 3 shows the propagation loss measurements for SiPSi waveguides with dimensions W x H = 4 x 2μm that have been oxidized in the same way as the SOI waveguides mentioned above. The measured losses were 2.1±0.2dB/cm at 1.55μm and 3.9±0.2dB/cm at 3.39μm.

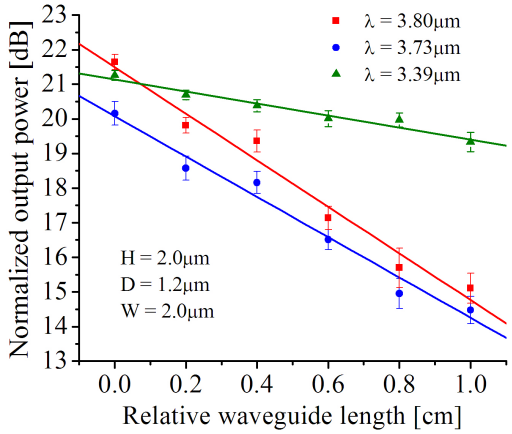

Fig. 1. – SOI rib waveguide propagation loss measurements.

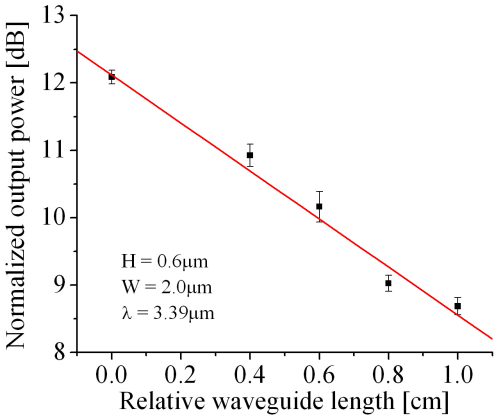

Fig. 2. Propagation losses for silicon-on-sapphire [8]. Losses were 3.6±0.2dB/cm.

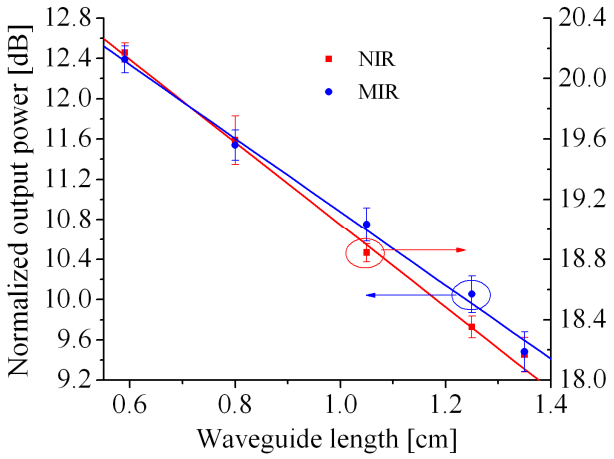

Fig. 3. Propagation loss measurements for oxidized SiPSi waveguides for NIR and MIR [4]. Losses were 2.1±0.2dB/cm at 1.55μm and 3.9±0.2dB/cm at 3.4μm.

3. FREE-CARRIER PLASMA DISPERSION EFFECT CALCULATIONS

In near-infrared silicon photonic the plasma dispersion effect has become the most commonly used modulation mechanism. By changing the number of free charge-carriers in a waveguide core, either through injection or depletion, the refractive index and absorption coefficient of the waveguide can be altered.

Classical Drude-Lorentz theory models the magnitude of these changes in absorption coefficient and refractive index as being proportional to the square of the wavelength. However, due to a number of simplifying assumptions in this theory [11] the Drude equations serve only as an estimate of the plasma dispersion effect, and a different approach should be taken to produce accurate equations that could be used in modeling devices that exploit this effect.

Soref and Bennett produced equations that relate the change in absorption coefficient $\Delta\alpha$ and refractive index Δn to the change in concentrations of electrons, ΔN_e, and holes, ΔN_h, in silicon at the wavelengths 1.3μm and 1.55μm [12]. Their use has become widespread and has been successfully used in a range of telecoms wavelength modulators [13-15]. They took a semi-empirical approach, where change in absorption coefficient spectra were first calculated from absorption coefficient spectra of heavily doped silicon wafers from literature. Refractive index change spectra were then calculated from these absorption coefficient spectra using the Kramers Kronig relations, which relate the absorption coefficient of a material to its refractive index [12]:

$$\Delta n(\omega) = (c/\pi) P \int_0^\infty \frac{\Delta\alpha(\omega')\, d\omega'}{\omega'^2 - \omega^2} \tag{1}$$

where $\hbar\omega$ is the photon energy. P indicates that the principal part must be taken, as there is a singularity at $V'=V$. We can rewrite (1) in terms of normalized photon energy V, where $V = \hbar\omega/e$:

$$\Delta n(V) = 6.3\times10^{-6}\ P \int_0^\infty \frac{\Delta\alpha(V')\, dV'}{V'^2 - V^2} \tag{2}$$

The above expression can be calculated using a numerical approach that applies a trapezoidal rule approximation [16]. Although theoretically the integration should be performed over all photon energies from 0 to ∞, at low photon energies free-carrier absorption saturates, and at high photon energies the absorption spectra of the doped wafers meet the curve of the intrinsic spectrum, closing off the integral at a finite value.

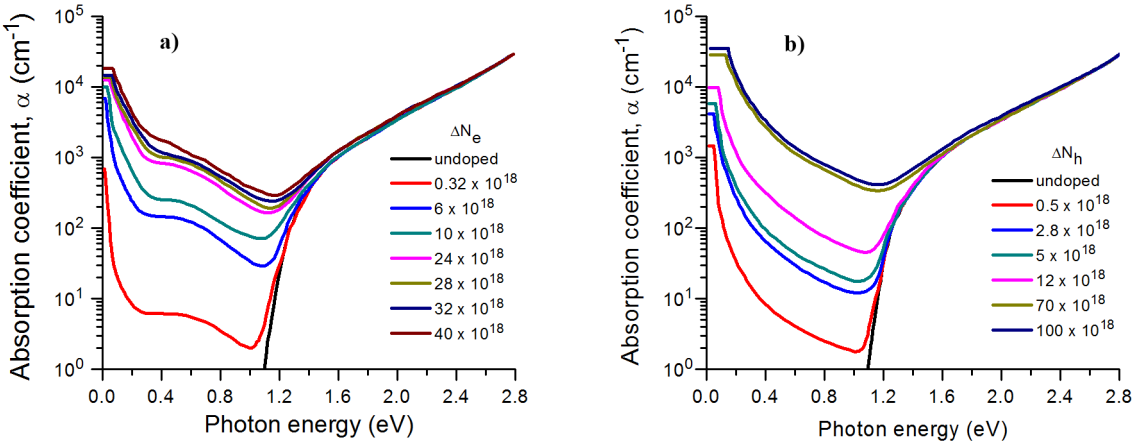

Fig. 3. Absorption coefficient spectra of heavily doped silicon wafers a) n-type b) p-type.

The absorption spectra used for these calculations are a composite of numerous existing literature data sets, which we have listed elsewhere [17]. Figures 3a and 3b show these composite absorption spectra for p- and n-type silicon respectively.

Figures 4 and 5 show the change in refractive index spectra that are calculated from the data in figures 3a and 3b using equation (2).

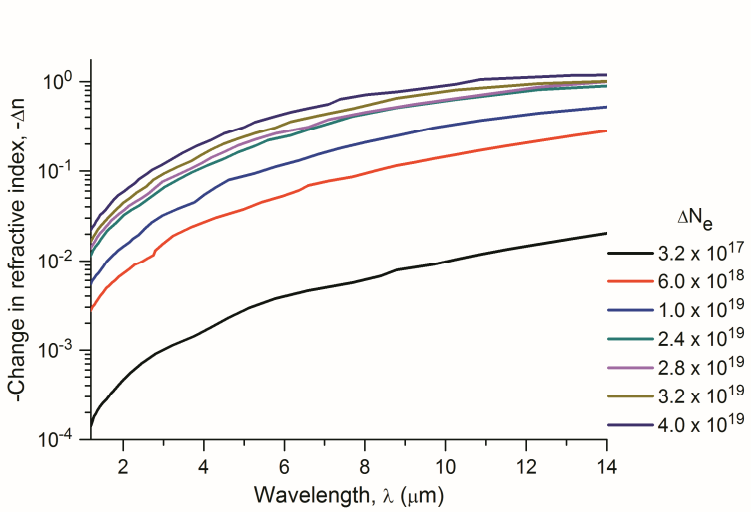

Fig. 4. Change in refractive index spectra for heavily doped n-type silicon samples in the 1.2-14μm wavelength range.

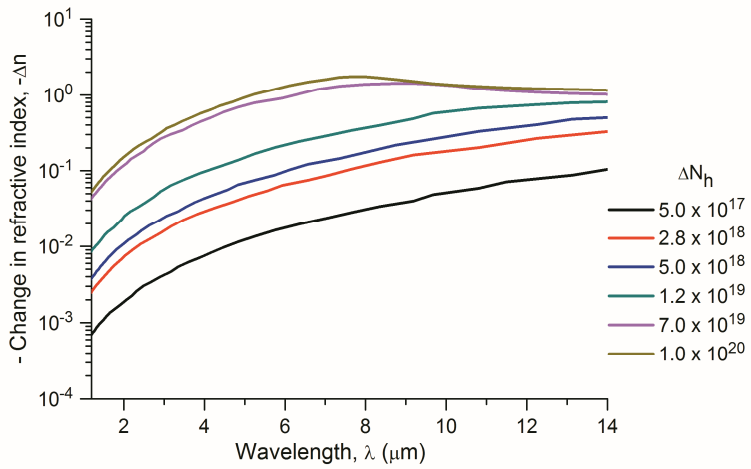

Fig. 5. Change in refractive index spectra for heavily doped p-type silicon samples in the 1.2-14μm wavelength range.

From this data we have produced expressions that link $\Delta\alpha$ and Δn to ΔN_e and ΔN_h at specific wavelengths from 1.2 to 14μm. Equations (3) and (4) give the general forms of these equations, and table 1 gives the coefficients to be substituted into these equations at specific wavelengths, λ.

$$\Delta\alpha(\lambda) = \Delta\alpha_e(\lambda) + \Delta\alpha_h(\lambda) = a(\lambda)\Delta N_e^{\,b(\lambda)} + c(\lambda)\Delta N_h^{\,d(\lambda)} \tag{3}$$

$$-\Delta n(\lambda) = \Delta n_e(\lambda) + \Delta n_h(\lambda) = p(\lambda)\Delta N_e^{\,q(\lambda)} + r(\lambda)\Delta N_h^{\,s(\lambda)} \tag{4}$$

where a, b, c, d, p, q, r and s are coefficients that can be found in Table 1 for different λ.

Table 1. Coefficients for $\Delta\alpha$ vs. ΔN and $-\Delta n$ vs. ΔN equations at wavelengths from 1.3μm to 14μm. Coefficients c and d hold at $\lambda \geq 11$ μm for $\Delta N_h \leq$ 1.2E19, p and q hold at $\lambda \geq 9$ μm for $\Delta N_e \leq$ 1E19 and r and s hold at $\lambda \geq 8$ μm for $\Delta N_h \leq$ 1.2E19.

Wavelength, λ (μm)	Δα				-Δn			
	a (cm^2)	b	c (cm^2)	d	p (cm^3)	q	r (cm^3)	s
1.3	3.48E-22	1.229	1.02E-19	1.089	2.98E-22	1.016	1.25E-18	0.835
1.55	8.88E-21	1.167	5.84E-20	1.109	5.40E-22	1.011	1.53E-18	0.838
2.0	3.22E-20	1.149	6.21E-20	1.119	1.91E-21	0.992	2.28E-18	0.841
2.5	1.67E-20	1.169	8.08E-20	1.123	5.70E-21	0.976	5.19E-18	0.832
3.0	6.29E-21	1.193	3.40E-20	1.151	6.57E-21	0.981	3.62E-18	0.849
3.5	3.10E-21	1.210	6.05E-20	1.145	6.95E-21	0.986	9.28E-18	0.834
4.0	7.45E-22	1.245	5.43E-20	1.153	7.25E-21	0.991	9.99E-18	0.839
4.5	2.16E-22	1.277	5.58E-20	1.158	1.19E-20	0.985	1.29E-17	0.838
5.0	9.28E-23	1.299	6.65E-20	1.160	2.46E-20	0.973	2.03E-17	0.833
5.5	4.58E-23	1.319	8.53E-20	1.159	3.64E-20	0.968	3.31E-17	0.826
6.0	3.26E-23	1.330	1.53E-19	1.149	4.96E-20	0.965	6.92E-17	0.812
6.5	2.70E-23	1.338	1.22E-19	1.158	5.91E-20	0.964	8.23E-17	0.812
7.0	2.25E-23	1.345	1.29E-19	1.160	5.52E-20	0.969	1.15E-16	0.807
7.5	1.36E-23	1.359	9.99E-20	1.170	3.19E-20	0.984	4.81E-16	0.776
8.0	1.85E-23	1.354	1.32E-19	1.167	3.56E-20	0.984	7.44E-16	0.769
8.5	3.05E-23	1.345	1.57E-18	1.111	8.65E-20	0.966	7.11E-16	0.774
9.0	4.08E-23	1.340	1.45E-18	1.115	2.09E-19	0.948	5.29E-16	0.783
9.5	4.14E-23	1.341	1.70E-18	1.115	2.07E-19	0.951	9.72E-16	0.772
10.0	3.81E-23	1.344	1.25E-18	1.125	3.01E-19	0.944	1.22E-15	0.769
10.5	4.23E-23	1.344	8.14E-19	1.137	5.07E-19	0.934	1.16E-15	0.772
11.0	5.81E-23	1.338	1.55E-18	1.124	1.51E-19	0.965	3.16E-15	0.750
11.5	8.20E-23	1.331	4.81E-18	1.100	2.19E-19	0.958	1.51E-14	0.716
12.0	1.13E-22	1.325	4.72E-18	1.102	3.04E-19	0.953	2.71E-14	0.704
12.5	1.22E-22	1.324	2.09E-18	1.124	4.44E-19	0.945	2.65E-14	0.706
13.0	1.09E-22	1.328	1.16E-18	1.140	6.96E-19	0.936	2.94E-14	0.705
13.5	1.20E-22	1.327	2.01E-18	1.130	1.05E-18	0.928	6.85E-14	0.686
14.0	1.62E-22	1.321	7.52E-18	1.101	1.45E-18	0.922	2.60E-13	0.656

4. DISCUSSION

4.1. Waveguide loss measurements

For SOI waveguides we have measured losses of 2.0-2.4dB/cm at 3.39μm, 2.9±0.3dB/cm at 3.73μm and 3.4±0.2dB/cm at 3.80μm - clearly the losses are increasing with wavelength. At 3.39μm we saw that the loss decreased to only 0.6-0.7dB/cm after sample oxidation, suggesting that a large part of these losses is due to optical mode interaction with sidewall roughness. Therefore at longer wavelengths, where we would expect the mode size to increase, we would expect to see some increased scattering loss. These results appear to confirm absorption coefficient measurements of bulk SiO_2 [2] that tell us that the loss increases just below 4μm. However at 3.8μm this loss is still quite tolerable and indicates that SOI will be the material platform of choice through most of the 3-4μm range.

We have also fabricated and characterized SOS and SiPSi for wavelengths longer than this, where alternatives to SiO_2 must be found for the lower cladding layer of waveguides. At 3.39μm we measured losses of 3.6±0.2dB/cm for SOS and 3.9±0.2dB/cm for SiPSi. For the SiPSi waveguides the loss at 3.39μm is nearly 2dB/cm greater than the loss at 1.55μm, which suggests that for these waveguides, as with the SOI rib waveguides discussed above, roughness scattering loss is a major loss mechanism. Absorption loss measurements of porous silicon for MIR would be needed to confirm this. It is expected that through improvements in the fabrication processes the loss of these waveguides could be reduced, and both material platforms look like good candidates for further investigation at longer wavelengths.

4.2. Silicon free-carrier electroabsorption and electrorefraction predictions for MIR wavelengths

We hope that the calculated predictions for the absorption coefficient and refractive index changes due to the presence of free charge-carriers will be useful to future designers of components such as modulators for the infrared by enabling accurate device modeling. More broadly, the results of these calculations have implications for modulator design at longer wavelengths. Electro-absorption (the change in absorption coefficient induced by charge-carriers) becomes

dominant compared to electro-refraction at longer wavelengths. For example, at 8μm the π-phase shift length is predicted to be 70μm with a charge-carrier concentration of $\Delta N_e = \Delta N_h = 1E18$. In a waveguide of this same length with the same charge-carrier concentration the absorption loss is predicted to be 4.4dB [11]. In a Mach-Zehnder modulator absorption loss in either arm degrades the device performance, so that at wavelengths above 4μm it is no longer viable, but a simple device based on carrier-injection into a straight waveguide becomes a useful intensity modulator.

5. CONCLUSIONS

We have shown that SOI is a useful material for integrated group IV photonics in the 3-4μm wavelength range, where we have fabricated and characterized SOI rib waveguides with <1dB/cm propagation loss. We have also shown that silicon-on-sapphire and silicon-on-porous silicon are viable material platforms in the mid-infrared, and for each waveguide type have measured waveguides with loss <4dB/cm at 3.39μm. These two material platforms offer good replacements for SOI in those regions of the MIR spectrum where SiO_2 has high absorption.

We have also presented predictions for electroabsorption and electrorefraction using the free charge-carrier plasma dispersion effect over the 1.3-14μm wavelength range. These predictions are expected to be useful in the design of mid-infrared modulators, and suggest that electroabsorption modulators will be more effective at wavelengths higher than 4μm.

ACKNOWLEDGEMENTS

This work was supported by the Royal Society through the Royal Society Research Fellowship and by the EPSRC "UK Silicon Photonics" grant. Richard Soref appreciates the sponsorship of his work by the Air Force Office of Scientific Research (Gernot Pomrenke, Program Manager) under Grant FA9550-10-1-0417.

REFERENCES

[1] Soref, R.A., "Mid-infrared photonics in silicon and germanium," *Nature Photonics* 4, 495-497 (2010).
[2] Soref, R.A., "Towards silicon-based longwave integrated optoelectronics," *Proc. SPIE* 6898, 6898-09 (2008).
[3] Soref, R. A., Emelett, S. J., and Buchwald, W. R., "Silicon waveguided components for the long-wave infrared region," *J. Opt. A: Pure Appl. Opt.* 8, 840-848 (2006).
[4] Milošević, M. M., Thomson, D. J., Chen, X., Cox, D., and Mashanovich, G. Z., "Silicon waveguides for the 3-4 μm wavelength range," *8th IEEE Group IV Photonics conference*, London, UK, 14-16 September 2011.
[5] Baehr-Jones, T., Spott, A., Ilic, R., Penkov, B., Asher, W., and Hochberg, M., "Silicon-on-sapphire integrated waveguides for the mid-infrared," *Opt Express* 18(12), 12127-12135 (2010).
[6] Li, F., Jackson, S., Grillet, C., Magi, E., Hudson, D., Madden, S. J., Moghe, Y., O'Brien, C., Read, A., Duvall, S. G., Atanackovic, P., Eggleton, B. J. and Moss, D., "Low propagation loss silicon-on-sapphire waveguides for the mid-infrared," *Opt Express* 19(16), 15212-15220, 2011.
[7] Spott, A., Liu, Y., Baehr-Jones, T., Ilic, R., and Hochberg, M., "Silicon waveguides and ring resonators at 5.5μm," *Appl. Phys. Lett.* 97(21), 213501 (2010).
[8] Mashanovich, G. Z., Milošević, M. M., Nedeljkovic, M., Owens, N., Xiong, B., Teo, E. J., and Hu, Y., "Low loss silicon waveguides for the mid-infrared," *Opt Express* 19(8), 7112-7119 (2011).
[9] Wei, Y., Li, G., Hao, Y., Li, Y., Yang, J., Wang, M. and Jiang, X., "Long-wave infrared 1 x 2 MMI based on air-gap beneath silicon rib waveguides," *Opt. Express* 19(17), 15803-15809 (2011).
[10] Milošević, M. M., Matavulj, P. S., Yang, P.Y., Bagolini, A. and Mashanovich, G. Z., "Rib waveguides for mid-infrared silicon photonics," *J. Opt. Soc. Am. B*, 26(9), 1760-1766 (2009).
[11] Nedeljkovic, M., Soref, R. A., and Mashanovich, G. Z., "Free-carrier electro-absorption and electro-refraction modulation in group IV materials at mid-infrared wavelengths," *Proc. SPIE 8266*, 82660Y (2012).
[12] Soref, R. A., and Bennett, B. R., "Electrooptical effects in silicon," *IEEE J. Quantum Electronics*. 23(1), 123-129 (1987).
[13] Reed, G. T., Mashanovich, G., Gardes, F. Y., Thomson, D. J., "Silicon optical modulators," *Nature Photonics* 4, 518-526 (2010).
[14] Thomson, D. J., Gardes, F. Y., Hu, Y., Mashanovich, G., Fournier, M., Grosse, P., Fedeli, J-M., and Reed, G. T., "High contrast 40Gbit/s optical modulation in silicon," *Opt Express* 19(12), 11507–11516 (2011).

[15] Gardes, F. Y., Thomson, D. J., Emerson, N. G., and Reed, G. T., "40 Gb/s silicon photonics modulator for TE and TM polarisations," *Opt Express* 19(12), 11804-111814 (2011).
[16] Collocott, S. J., and Troup, V, "Adaptation: numerical solution of the Kramers-Kronig transforms by trapezoidal summation as compared to a Fourier method," *Computer Physics Communications* 17, 393-395 (1979).
[17] Nedeljkovic, M., Soref, R. A. and Mashanovich, G. Z., "Free-carrier electro-absorption and electro-refraction modulation predictions for silicon over the 1-14μm infrared wavelength range," *IEEE Photonics Journal* 3(6), 1171-1180 (2011).